INSTITUTE FOR AEROSPACE STUDIES

UNIVERSITY OF TORONTO

A THEORETICAL ANALYSIS OF THE DRIVER-RESERVOIR METHOD OF DRIVING HYPERSONIC SHOCK TUNNELS

by

Robert F. Flagg

APRIL 1965

UTIAS TECHNICAL NOTE NO. 93

A THEORETICAL ANALYSIS OF THE DRIVER-RESERVOIR METHOD OF DRIVING HYPERSONIC SHOCK TUNNELS

by

Robert F. Flagg

APRIL 1965 UTIAS TECHNICAL NOTE NO. 93

ACKNOWLEDGEMENTS

I wish to express my thanks to Dr. G. N. Patterson for the opportunity to continue this work at the Institute for Aerospace Studies. I wish also to express my appreciation to the AVCO Research and Advanced Development Division of Wilmington, Massachusetts for permission to release that part of the work which was conducted during my affiliation with them. I am also indebted to Mr. H. Weisblatt under whose supervision this research was initiated at AVCO-RAD and to Dr. I. I. Glass whose continued interest and guidance is gratefully acknowledged.

The work was supported by the Defence Research Board of Canada and by the U. S. Air Force under contract number ARL-AF-33(615)-2766.

SUMMARY

The driver-reservoir method of extending the test time of a tailored hypersonic shock tunnel by using a reservoir and a nozzle (perforated plate) at the upstream end of the driver is treated theoretically. It is shown that the flow following the rupture of the diaphragm is highly complex and contains both steady and unsteady flow regimes. It is also shown that the area ratio of the nozzle separating the driver from the reservoir determines the nature of the wave system produced. For a unique or "ideal" nozzle area ratio a flow system is produced which contains no downstream running disturbances other than Mach waves. That is, both the head and the tail of the initial rarefaction wave are prevented from interfering with the shock-tunnel reservoir. Consequently, the running time of the shock tunnel can be extended. The ideal area ratios are calculated for a wide range of shock tunnel operating conditions and compared with experimental results. The comparison shows that the ideal nozzle area ratio can be predicted accurately from theory.

TABLE OF CONTENTS

NOTATION

A	area
a	speed of sound
C_p	specific heat at constant pressure
f	"tailoring constant"
g	"cross-over constant"
m	molecular weight
M	Mach wave
M_f	flow Mach number
M_S	shock Mach number
M_{S_T}	tailored shock Mach number
M_{S_x}	cross-over shock Mach number
p	pressure
P	defined by Eq. 1
$\overleftarrow{R}$	left (upstream) running unsteady expansion
$\overrightarrow{R}$	right (downstream) running unsteady expansion
$\mathcal{R}$	universal gas constant
$\overleftarrow{S}$	left (upstream) running shock
$\overrightarrow{S}$	right (downstream) running shock
$\overrightarrow{S_i}$	incident shock
T	temperature
t	time
u	velocity

ρ	density
γ	specific heat ratio
δ	ratio of nozzle minimum area to tube cross section area (A^*/A_1)
δ_{IDEAL}	area ratio which produces no right (downstream) running disturbances (except a Mach wave)
$\delta_{\overrightarrow{R}}$	area ratio which produces a single right (downstream) running unsteady expansion
$\delta_{\overrightarrow{S}}$	area ratio which produces a single right (downstream) running shock
$(\ )^*$	conditions at nozzle minimum area
$(\ )_1$	driven section initial conditions
$(\ )_2$	conditions behind a moving normal shock
$(\ )_{3u}$	conditions in unsteady expanded driver
$(\ )_{3s}$	conditions in steady expanded river
$(\ )_4$	driver initial conditions
$(\ )_5$	conditions behind reflected normal shock
$(\ )_o$	stagnation conditions
$(\ )_s$	conditions at shock front
$(\ )_x$	cross-over conditions
$(\ )_{ij}$	$(\ )_i/(\ )_j$

1. INTRODUCTION

One limitation to the duration of the steady state reservoir condition of a tailored hypersonic shock tunnel is the arrival of the head of the rarefaction wave which has been reflected from the upstream end of the driver as in Figure 1. This reflected wave, which results from the bursting of the diaphragm, cannot be eliminated directly but can be controlled to advantage. For example, the quasi-steady test time may be increased simply by lengthening the driver to a value such that the reflected rarefaction wave does not arrive at the downstream reflecting surface until after a given period of time. The driver length cannot be extended indefinitely since the limit to the test time may then be determined by the arrival of the tail of the rarefaction wave. The optimum test time for a given geometry occurs when both the head and the tail of the rarefaction arrive simultaneously at the reflecting surface. This point is discussed in detail by Holder and Schultz in Reference 1. Further gains in test time can only be obtained by lengthening the overall length of the entire tube while preserving the driver to driven length proportion. This raises the practical problem of space and cost since relatively long sections are required if tunnel test time is to be increased significantly.

Another technique for increasing the tunnel test time is the so-called driver-reservoir technique suggested by Henshall, Teng, and Wood (Ref. 2). They demonstrated experimentally that this method can significantly increase the shock tunnel running time. However, the physical model used to explain the results is in error. They suggested that since the closed end of a shock tube reflects a disturbance of the same sense as the incident disturbance, (shocks reflect as shocks and rarefactions reflect as rarefactions) and that an open end reflects a disturbance of the opposite sense (shocks reflect as rarefactions and rarefactions reflect as shocks) that there would exist a partially opened-partially closed configuration that would produce a Mach wave i.e., a vanishingly small disturbance for a given set of initial conditions, analogous to the steady transonic tunnel case. However, it will be shown subsequently that, in general, a very complex flow containing both steady and unsteady flow regimes is generated and for a unique nozzle area ratio a flow system is possible which contains no downstream running disturbances. Hence the running time of a hypersonic shock tunnel may be increased without recourse to extension of the length of the facility.

2. SOME BASIC CONSIDERATIONS

The essence of the driver reservoir problem is the interaction of rarefaction wave with a perforated plate separating a constant area duct and a large volume. In Ref. 3 the equivalence between a perforated plate or wire grid of a given open to closed area ratio and a nozzle of the same ratio was established. In Ref. 4 it was shown from chambered shock tube theory that for cross - section area ratios greater than about 6, the results of an area change are essentially those obtained from an infinite area

ratio. Hence, the reservoir can be assumed to be infinite in diameter with little loss in generality. The prototype and the flow system to be analyzed are shown schematically in Fig. 2.

A partial analogy exists between the driver-reservoir case and the case of colliding unsteady expansions. Recall that the solution to the problem of two colliding rarefaction waves can be obtained either by using the method of characteristics in the (x, t)-plane wherein all of the details including the interaction region are laboriously calculated or by applying the simpler (p, u)-plane analysis to predict what final disturbances will emerge from the collision. The latter approach is considerably less involved and yields all of the required information for the resulting quasi-steady states. However, no details of the interaction region can be obtained in this manner. For the (p, u)-plane analysis the appropriate equations are applied to solve the problem "in the large". A discussion of such interaction problems is given in Refs. 5 and 6.

A similar approach can be used in the driver-reservoir flow problem. That is, a solution can be obtained either by analyzing the complex interaction region using the laborious method of characteristics in the (x, t)-plane or by moving away from the interaction region and with the aid of a simpler (p, u)-plane analysis and the appropriate steady and unsteady flow equations, obtaining an analytic algebraic solution for the disturbances that finally emerge from the interaction region.

This type of analysis in effect neglects the effects of secondary interactions of characteristic lines. As shown by Bird (Ref. 7) this assumption is valid as long as the wave strengths are not extreme. The neglect of secondary characteristic interactions implies that a definite wave pattern bounding quasi-steady regions finally emerges from the interactions. It will be shown later that the experimental data agrees well with the simplified theoretical approach hence the neglect of secondary disturbances appears to be a reasonable assumption.

3. EXPANSION PROCESSES

When the diaphragm separating the driver and driven sections opens, the gas in the driver (the term "driver" will be restricted to the regions between the diaphragm and the perforated plate) undergoes an unsteady expansion to a new state (3 u) Fig. 1, which is fixed by the initial conditions in both driver and driven sections. The gas flowing through the nozzle or perforated plate ultimately undergoes a steady expansion to a condition (3s), which is fixed by the area ratio and is governed by the steady flow relations. Since the physical properties of these two expansions are very different, some "patching" of these two processes is necessary in terms of additional unsteady waves to satisfy the boundary conditions imposed by each flow. It is essentially these "patching" solutions which provide the basis for theory of the driver-reservoir technique.

An isentropic expansion of a perfect gas may be either steady or unsteady. The unsteady isentropic expansion of the driver gas is such that the pressure distribution in the driver (Fig. 1) will be changing with time. For the backward (left) facing rarefaction wave $\overleftarrow{R}$, a quantity P defined by (Ref. 5)

$$P = \frac{2}{\gamma - 1} a + u \tag{1}$$

is constant across the unsteady expansion and provides the relation between thermal and directed motion. The pressure ratio across an unsteady expansion where the gas is initially at rest may be written as

$$\frac{p_{3u}}{p_4} = \left[1 - \frac{(\gamma_4 - 1) u_{3u}}{2 a_4} \right]^{\frac{2\gamma_4}{\gamma_4 - 1}} \tag{2}$$

The steady isentropic expansion of the reservoir gas through the nozzle produces a pressure distribution which after the initial starting transient is invariant with time. The steady flow energy equation provides the counterpart of Eq. 1, and is expressed by

$$C_p \bar{T}_o = C_p T + \frac{u^2}{2} \tag{3}$$

The pressure ratio across an isentropic steady expansion, where the gas is initially at rest, follows from Eq. 3, and is given by

$$\frac{p_{3s}}{p_4} = \left[1 - \frac{(\gamma_4 - 1)}{2} \left(\frac{u_{3s}}{a_4} \right)^2 \right]^{\frac{\gamma_4}{\gamma_4 - 1}} \tag{4}$$

Note that Eqs. (2) and (4) are not in general equal and that a given initial state expanded to a given velocity by both methods will not yield the same temperature or pressure. The properties of the two expansion flows are shown clearly in the (p, u)-plane on Fig. 3.

From Fig. 3 it is seen that there is only one point other than the initial state where the two expansions will produce the same end state. This unique state is found by equating Eqs. (2) and (4) giving

$$\left[1 - \frac{(\gamma_4 - 1) u_{3u}}{2 a_4} \right]^2 = 1 - \frac{\gamma_4 - 1}{2} \left(\frac{u_{3s}}{a_4} \right)^2 \tag{5}$$

Solving for u yields:

$$\frac{u_3}{a_4} = \frac{4}{\gamma_4+1} \qquad M_3 = \frac{4}{3-\gamma_4} \tag{6}$$

It is worth noting that a detailed analysis of the conditions at this point (the "cross-over" point) and their compatability with the tailoring constraint is done in Appendix A. The results show that very stringent requirements are placed on the initial conditions if both tailoring and cross-over conditions are to be satisfied simultaneously. (The problem is trivial if only the cross-over condition is specified (i.e. nontailored operation) since the shock tube initial conditions may be readily adjusted to yield this value. However it is assumed throughout this paper that tailored operation is implied.) Appendix A demonstrates that the conventional shock-tunnel driving methods i.e. hydrogen drivers, helium drivers and combustion drivers will not satisfy both of these requirements simultaneously. In fact for air as the driven gas only a driver gas having a specific heat ratio of 1.18 will satisfy this requirement for perfect gases.

Additional disturbances, shocks or expansions or combinations of the two, will be necessary to "patch" the steady and unsteady flow regimes, for the general case.

4. POSSIBLE WAVE SYSTEMS

The problem of determining the wave systems which will patch the two expansion flows for a tailored condition reduces to the following. A point (A) (the so-called right state of Ref. 5) as in Fig. 3, is specified on the unsteady expansion curve corresponding to the tailored condition. A nozzle area ratio is chosen for the steady expansion curve, hence a point (B) (the so-called left state of Ref. 5) is specified on the steady expansion curve. These two points must now be connected by some additional unsteady disturbances, such as left or right running shocks, left or right running rarefactions, Mach waves or combinations of these.

There are many combinations that can be hypothesized from these disturbances. However, most of them are "unstable", that is, they consist of over-taking waves which would have to originate (at infinity) prior to the interaction hence violate the initial collision conditions (at $t = 0$) of the problem. Several "stable" transitions do exist. Stable transitions are those in which no change in the character of the patching wave system occurs with time, that is the waves are receding from the interaction. It should be noted

that any right running wave arising from the above wave system will ultimately overtake the incident shock if the tube is sufficiently long. However, it will be assumed that the tube is short enough in that the incident shock reflects from the end of the tube before any overtaking occurs. It will be shown later that only cases that contain no right running waves are of interest hence this point is of little interest.

An additional restriction must be imposed on some wave systems, since the strength of the left (upstream) running wave must be such that it either stands still in the laboratory coordinates or is swept downstream to the right. The restriction to be satisfied is

$$M_{F_E} \geq M_S'$$

where, M_{F_E} is the flow Mach number evaluated at the nozzle exit and M_S' is the shock Mach number of the upstream running shock based on a shock velocity taken with respect to the velocity and sound speed of the gas just upstream of the shock. Shocks of greater strength would propagate upstream into the nozzle and break down the flow, hence are "unstable".

The patching waves which emerge from the interaction region are the result of the collision of rarefaction waves and compression waves which are generated when the initial left running rarefaction first interacts with a decreasing area ratio (the exit (right Fig. 2) side of the nozzle) and the transmitted rarefaction wave interacts with an increasing area ratio (the entrance (left) side of the nozzle). A second interaction occurs when the disturbance generated at the entrance side of the nozzle, moves downstream through the exit of the nozzle. The detailed nature of the interactions can only be obtained by using the method of characteristics. The final emergent wave systems is the product of several basic shock (compression wave) and rarefaction wave interactions.

In references 8 and 9 these basic interactions are discussed. It is shown (ref. 8) that for real gases the overtaking of a rarefaction wave by a shock (compression wave) always results in a reflected shock and a transmitted rarefaction wave if the overtaking shock is weak, and a transmitted shock if the overtaking shock is strong. In ref. 9 it is shown that in the case of the overtaking of a shock wave by a rarefaction wave both reflected shock waves and rarefaction waves are possible. If the overtaking rarefaction is weak then the transmitted wave is a shock wave; if it is strong then transmitted rarefaction wave results.

Since at the nozzle both of these cases can exist, it can readily be shown that 9 stable configurations are possible (counting the 5

limiting cases which have transmitted or reflected Mach waves), as shown in Table 1.

Which of the nine stable systems occurs in a given situation depends on two parameters; the ratio of the tailored shock Mach number to cross over shock Mach number (M_{S_T}/M_{S_x}), and the ratio of the actual nozzle area ratio to an ideal nozzle area ratio (δ/δ_{IDEAL}), that is, there will be three distinct cases which depend on whether the tailored condition occurs at a lower, identical to, or higher velocity than the cross over velocity and for each of these three cases there will be different subcases produced depending on whether the nozzle area ratio is larger, identical to, or smaller than the ideal value.

Case 1 $\quad M_{S_T}/M_{S_x} < 1$

For this case the tailored conditions occurs at a lower velocity or shock Mach number than does the cross-over condition. (Methods of finding the tailored and cross-over conditions are given in ref. 10 and Appendix A respectively.)

This is the case usually found in practice and is representative of the more common modes of operation, He/Air, H_2/Air, Combustion gases/Air. The possible wave systems are indicated on the (p, u)-plane of Fig. 4, and are tabulated in Table 1. For no nozzle i.e. $\delta = 1$ the matching is accomplished by a single left running rarefaction wave and right running shock wave (wave system 3). This right running shock will ultimately reach the shock tunnel reservoir region and increase the reservoir pressure signaling the end of the steady running conditions. As the nozzle size is decreased the strength of both the left running rarefaction and right running shock are decreased. When $\delta = \delta_S$ a single right running shock is sufficient to join the two flow regimes (wave system 6). A further decrease in nozzle area ratio gives rise to left and right running shocks (wave system 9, the right running shock decreasing in strength as the left one increases in strength. As δ approaches δ_{IDEAL} the right running shock become progressively smaller and vanishes in the limit and the matching is accomplished by a single left (upstream) running shock (wave system 8). It is important to note that in this limit there are no right running disturbances other than Mach waves being produced in the flow (except for the original incident shock). Hence, no waves are available which could alter the steadiness of the shock tunnel reservoir. The initial rarefaction wave has been replaced by a steady expansion, a single left running shock and Mach waves. If the nozzle area ratio decreases further, non-ideal operation again occurs in that matching is accomplished by a left running shock wave and a right running rarefaction wave (wave system 7). The right running rarefaction

will ultimately propagate into the reservoir region and decrease the reservoir pressure and signal the end of the steady reservoir conditions. The static pressure profiles produced along the tube for the several types of waves systems, are included in Fig. 4.

Case 2 $M_{S_T}/M_{S_X} = 1$

This case is not usually found in practice but is included for completeness. It corresponds to the case where the tailored condition and the cross over condition occur at the same state. It is the simplest of the three cases to analyse and is closest to the explanation put forward in ref. 2. The possible wave diagrams are shown in Fig. 3 and tabulated in Table 1. For $\delta = 1$, matching is accomplished through a left running rarefaction and a right running shock (wave system 3). As in the previous case the right running shock will propagate into the reservoir region and end the steady tunnel reservoir time. As δ is decreased both the shock and the expansion weaken till in the limit as δ approaches δ_{IDEAL} both vanish simultaneously (wave system 5), leaving no disturbances in the flow. The steady and unsteady expansions are now matched together without that aid of any additional disturbances. This is the ideal situation for the $M_{S_T} = M_{S_X}$ case. If δ is further decreased, the roles of the shock and rarefaction are interchanged, the shock propagating upstream and the rarefaction propagating downstream into the reservoir region, and eventually lowering the reservoir pressure (wave system 7). The static pressure profiles along the tube for this case are included in Fig. 5.

Case 3 $M_{S_T}/M_{S_X} > 1$

This case is not generally attained in practice but is included since it may be of further interest in tailored chemical shock tubes where exotic gases or mixtures of gases are being investigated. The possible wave systems are indicated in Fig. 6 and are tabulated in Table 1. For nozzle $\delta = 1$, the matching is accomplished by a single left running rarefaction and a right running shock (wave system 3), a situation which will ultimately produce an increase in pressure in the shock tunnel reservoir region. As δ is decreased the strength of the left running shock decreases until as δ approaches δ_{IDEAL} which is also equal to δ_X for this case, matching is accomplished by a single upstream running rarefaction wave (wave system 2). The initial starting rarefaction has been replaced by a steady expansion, a left running rarefaction wave, and Mach waves. This is to be contrasted to the $M_{S_T}/M_{S_X}<1$ case where the matching in the ideal case was accomplished through the steady expansion and a left running shock. As δ is decreased further, the left running rarefaction wave decreases in strength until in the limit as δ approaches $\delta_R^{\uparrow}$ a single right running rarefaction wave is sufficient to join the flows (wave system 4). This character is symmetric to the $M_{S_T}/M_{S_X} < 1$ case where a single right running shock could match the two flows but for δ greater than δ_{IDEAL} rather than δ less than δ_{IDEAL}. If δ is further decreased, matching is ob-

tained by the addition of a left running shock (wave system 7). The pressure profiles for the above cases are also shown on Fig. 6.

In summary, it is found in general, that it takes two additional unsteady disturbances to match the steady flow of the reservoir gas with the unsteady flow of the driver gas. Further, there are special cases where only one disturbance is required, and what is very important is that it is possible to choose the nozzle area ratio to make this disturbance a left (upstream) running disturbance. This disturbance will be either a shock wave or a rarefaction wave depending on the ratio M_{S_T}/M_{S_X} and in the limit as this ratio approaches unity (i.e. the cross-over point) matching is accomplished automatically.

For all cases if the nozzle area ratio is made larger than the ideal value, right running shocks will propagate into the reservoir region and increase the reservoir pressure. Conversely, if the nozzle area ratio is made smaller than the ideal area ratio a rarefaction wave propagates into the reservoir region decreasing the reservoir pressure. This fact was observed in the experimental work of Ref. 2 and substantiates the present analysis.

It should be noted that the mass flow could have been used instead of the pressure in a "(m, u)-plane" analysis. However the features of the expansion flows in this plane are similar to the behaviour of them in the (p, u)-plane. Hence, to imply that the two flows can be patched if the mass flows are matched is not sufficient since equal mass flows does not imply equal pressures or velocities except, as has been shown above, at the cross-over point.

5. IDEAL NOZZLE AREA RATIOS

In the previous section it was shown that a wave system containing no right running disturbances of any kind can be obtained by expanding the gas in the reservoir through a steady expansion to a certain specific value, which is governed by the area ratio δ of the nozzle which is placed between the driver and reservoir regions.

It was specifically shown that for the cases $M_{S_T}/M_{S_X} = 1$ and $M_{S_T}/M_{S_X} > 1$ the ideal area ratio is the cross-over area ratio. For these two cases a simple exact result for the ideal nozzle area ratio can be obtained.

From steady isentropic flow theory, the nozzle area ratio is related to the flow Mach number by

$$\delta = M_{3_S}\left[\frac{2}{\gamma_4+1}\left(1+\frac{\gamma_4-1}{2}M_{3_S}^2\right)\right]^{-\frac{1}{2}\left(\frac{\gamma_4+1}{\gamma_4-1}\right)} \qquad (7)$$

Substituting into this relation the value of the flow Mach number at the cross-over point gives for the ideal nozzle area ratio:

$$\delta_{IDEAL} = \frac{4}{3-\gamma_4}\left[\frac{2(\gamma_4+1)}{(3-\gamma_4)^2}\right]^{-\frac{1}{2}\left(\frac{\gamma_4+1}{\gamma_4-1}\right)} \qquad \text{FOR} \quad \frac{M_{ST}}{M_{Sx}} \geq 1 \tag{8}$$

Note the interesting result that δ is a function of the driver gas ratio of specific heats only and is independent of all the other parameters. Values of δ are plotted in Fig. 7 and tabulated in Table 2 for the range of driver gas ratios of specific heat of interest.

For $M_{ST}/M_{Sx}<1$ the introduction of the upstream running matching shock complicates the system to the extend that no simple result for δ has been obtained to date. This is unfortunate since it is the case of immediate interest. The ideal area ratio can be calculated as follows. For a given γ_1, γ_4 and tailored shock Mach number, the corresponding diaphragm speed of sound ratio can be found from a simultaneous solution of four equations, as shown in Ref. 10. The area ratio δ may be found by using these four parameters as inputs to a system of equations which includes Eq. A-1 (Appendix A) evaluated at the tailored shock Mach number.

$$\frac{u_{3u}}{a_4} = \frac{2}{a_{41}(\gamma_1+1)}\left(M_{ST} - \frac{1}{M_{ST}}\right) \tag{9}$$

Equation 2 evaluated at the tailored velocity

$$\frac{P_{3u}}{P_4} = \left(1 - \frac{\gamma_4-1}{2}\frac{u_{3u}}{a_4}\right)^{\frac{2\gamma_4}{\gamma_4-1}} \tag{10}$$

the general shock velocity pressure ratio relation written for the left running matching shock

$$\frac{u_{3s}-u_{3u}}{a_4}\left(\frac{a_4}{a_3}\right) = \left[\frac{2}{\gamma_4(\gamma_4-1)}\right]^{\frac{1}{2}} \frac{\frac{P_{3u}}{P_4}\frac{P_4}{P_{3s}} - 1}{\left[1+\frac{\gamma_4+1}{\gamma_4-1}\frac{P_{3u}}{P_4}\frac{P_4}{P_{3s}}\right]^{\frac{1}{2}}} \tag{11}$$

the pressure ratio across the steady expansion as given by Eq. (4) above, the speed of sound ratio across the steady expansion given by

$$\frac{a_3}{a_4} = \left[1 - \frac{\gamma_4 - 1}{2}\left(\frac{u_{3S}}{a_4}\right)^2\right]^{\frac{1}{2}} \tag{12}$$

and an area-ratio-velocity relation for steady isentropic flow which may be expressed by

$$\delta = \left(\frac{\gamma_4+1}{2}\right)^{\frac{\gamma_4+1}{2(\gamma_4-1)}} \frac{u_{3S}}{a_4}\left[1 - \frac{\gamma_4+1}{2}\left(\frac{u_{3S}}{a_4}\right)^2\right]^{\frac{1}{\gamma_4-1}} \tag{13}$$

The procedure for finding δ consists of solving Eq. (9) for u_{3u}/a_4, substituting into Eq. (10) to obtain p_{3u}/p_4, then solving simultaneously Eqs. (11) and (4) for u_{3S}/a_4 using the auxiliary equation Eq. (12) for the speed of sound ratio. Finally u_{3S}/a_4 is inserted into Eq. (13) to yield δ .

This system of equations was solved numerically on the IBM 7090 using the above procedure. The results are presented in Fig. 8 and tabulated in Table 3.

From Fig. 8 it is noted that the ideal nozzle area ratio, δ_{IDEAL}, for the case M_{ST}/M_{Sx} is somewhat greater than δ_x depending on the tailored shock Mach number. The lowest shock Mach number shown here is 2.0 since at lower values the analysis begins to break down. For example $M_{ST} = 1$ implies a zero velocity of the unsteady expanded gas or no flow in the nozzle. As seen in Fig. 8, for increasing values of tailored Mach number the value of δ_{IDEAL} rapidly approaches δ_x from above. As a practical matter, as a first trial value to use in an experimental situation, the value of δ_x would usually suffice, the nozzle being enlarged as the results of the experiment dictate.

In this respect, it should be noted that the experimental value for hydrogen driving air ($\delta_{IDEAL} = 1/3$), as determined in Ref. 2, agrees very well with the exact value from this theory $\delta_{IDEAL} = 0.382$ and $\delta_x = 0.378$, considering that real gas effects, viscous effects, attenuation and secondary interactions are neglected.

Although the above has been derived for the tailored condition it is possible to operate "off-tailored" and still use the driver reservoir to extend the steady state shock tunnel reservoir time. In general, over-tailored operation ($M_S > M_{ST}$) requires a nozzle smaller than the ideal ($\delta < \delta_{IDEAL}$, see Fig. 4) and for "under-tailored" operation ($M_S < M_{ST}$) requires an area ratio larger than ideal. It may be seen from Fig. 8 that the value of δ_{IDEAL} changes very little, especially at the higher values of M_{ST}, consequently, the ideal nozzle area ratio will usually suffice even for the "off-tailored" conditions. This effect was verified if Ref. 2 where it is noted that within the accuracy of the experiment, δ_{IDEAL} was satisfactory ... a wide range of over and under-tailored conditions.

6. DRIVER-RESERVOIR TEST TIME LIMITS

Within the limits of the analysis it was shown that the driver-reservoir removes two of the test time limitations from shock tunnels, that of the arrival of the reflected head and tail of the rarefaction at the shock tunnel nozzle. However, test time limitations due to waves arriving at the nozzle do not vanish entirely since the unsteady matching disturbances which are being generated and propagated along the duct must be dealt with but later in time. New interfaces, and contact regions are being generated but since they are produced by nearly isentropic compression waves or at worst weak shocks their effect can usually be disregarded.

For the case where $M_{ST} = M_{Sx}$ and $\delta = \delta_{IDEAL}$, the limitation to the test time now is the arrival of a shock wave at the nozzle as can be seen from Fig. 9a (relevent wave systems shown in Table 1 are drawn symbolically for completeness since a detailed calculation by the method of characteristics has not been done). This wave is the end result of the incident shock being reflected first from the shock tube downstream and then travelling upstream to the reservoir nozzle and then again travelling downstream to the shock tunnel nozzle.

The resulting running time can be many times the original tailored test time for usual shock tube geometries. It must be noted that new test time limitations can now be imposed which are now more stringent than this, as by mass flow, radiative or convective heat loss considerations, for example.

For the case where $M_{ST}/M_{Sx} < 1$ and $\delta = \delta_{IDEAL}$, the matching between steady and unsteady expansion is made by a left running shock. Therefore, the limitation to the test time is now; the arrival at the shock tunnel reservoir region of the right-running rarefaction wave, which is generated by the collision of the original reflected shock and the upstream running patching shock as indicated in Fig. 9b. That this disturbance must be an expansion for all physically possible ratios of specific heat was shown in Ref. 11.

The expansion which limits the test time in this case was observed in Ref. 2. However, they incorrectly ascribed this to the original expansion being "delayed" at the reservoir. From a comparison of Fig. 9a and 9b it can be seen that the test time for this case will be greater than the original (no driver-reservoir) test time but will generally be less than that produced by the $M_{S_T}/M_{S_x} = 1$ case because the limiting disturbance is generated closer to the shock tunnel nozzle reservoir region. There is also an additional interface or interface region which is generated by the patching shock (see Table 1) which is not significant since it is found that the mismatch shock is relatively weak. However, if the nozzle and diaphragm stations are made coincident, then this second interface can be in principle, at least, be made coincident with the original interface and adjustment of the tailoring Mach number to a somewhat higher value will obscure this effect.

For $M_{S_T}/M_{S_x} > 1$ and $\delta = \delta_{IDEAL}$ the situation is similar in character to the $M_{S_T}/M_{S_x} < 1$ case except that shocks are replaced by expansions and visa versa. The end of the steady test time is signalled by the arrival of a shock or compression wave which is the result of the interaction of the reflected normal shock and upstream running patching rarefaction wave. This type of collision was analyzed in Ref. 7, and it is shown that the disturbance must be a shock or compression wave for all physically possible specific heat ratios. The wave diagram for this case is shown in Fig. 9c.

7. CONCLUSIONS

It has been shown that a complex flow containing both steady and unsteady flow regimes is produced by using the driver-reservoir technique to extend hypersonic shock tunnel running times. It is shown that by assuming the existence of a patching wave system that separate quasi-steady states, a solution can be obtained "in the large" by using a (p, u)-plane type of analysis. The results show that in general two additional disturbances separated by a contact surface are necessary to satisfy the boundary conditions imposed by the two different expansions. It is also shown that the actual flow pattern resulting from a given set of initial conditions is uniquely determined by the parameters M_{S_T}/M_{S_X} and δ/δ_{IDEAL}, where M_{S_T} is the tailored shock Mach number, M_{S_X} is the cross-over shock Mach number, δ is the given nozzle area ratio and δ_{IDEAL} is the nozzle area ratio which produces no downstream running waves. For a few special cases the flows can be joined with a single disturbance and for three unique cases corresponding to $M_{S_T} < M_{S_X}$, $M_{S_T} = M_{S_X}$, and $M_{S_T} > M_{S_X}$ an upstream running shock, a Mach wave, and an upstream running expansion respectively are produced. Since no downstream running disturbances (other than Mach waves) are contained in the flow, the shock-tunnel reservoir region will remain undisturbed for a longer period of time. In effect, the driver-reservoir when used ideally will replace the initial unsteady expansion by a steady expansion, an upstream running disturbance, and Mach waves, hence limitations due to both the reflected head and the tail of the original expansion are eliminated.

The ideal nozzle area ratio, which will produce this optimum condition (δ_{IDEAL}) is calculated for a wide range of conditions and compared with the available data. The agreement is very good considering that ideal, perfect gas flow is assumed throughout, and that secondary interactions of characteristics are neglected, and it lends support to the validity of these assumptions.

It is worth noting that a (p, u)-plane type of analysis is ideally suited for this type of problem, once it is assumed that quasi-steady states must exist after the interaction. However, it lacks the detail that a characteristics diagram in the (x, t)-plane provides. Consequently, it would be of value to do a characteristics solution in the (x, t)-plane for a few cases in order to establish precisely how the final wave system is generated. A comparison of the (p, u)-plane analysis (where secondary interactions were neglected) with a more exact analysis in ref. 7, shows good agreement as long as the wave strengths are not too large, which is generally the case in the present analysis.

The effect of driver length was not considered in the present problem. However, it can be seen that it is desirable to generate the final states in the neighbourhood of the driver reservoir.

In conclusion, it can be stated that the present analysis is

representative of the physical conditions and can be used with confidence to predict values of the ideal nozzle area ratio in order to extend the running times of a hypersonic shock tunnel.

REFERENCES

1. Holder, D.N. Schultz, D.L. — On the Flow in a Reflected Shock Tunnel, A.R.C. 22;52-Hyd. 130, (August, 1960) Also Progress in Astronautics and Aeronautics, Vol. 7, Hypersonic Flow Research, Academic Press, New York (1962).

2. Henshall, B.D. Teng, R.N. Wood, A.D. — A Driver-Sphere Technique for Increasing the Steady State Test Time of a Hypersonic Shock Tunnel, Proceedings of the Second Symposium on Hypersonic Technique, University of Denver, (20-21 March 1962), also Avco RAD-TM-62-16 (April 1962).

3. Benton, E.R. Knapton, D.A. — Supersonic Drag of Porous Wire Screens, A.R.S. Journal, Vol. 32, No. 10 (Oct. 1962).

4. Seigal, A.E. — The Influence of Chamber Diameter on the Muzzle Velocity of a Gun with an Infinite Length Chamber. NOL Navord Report 2691, (1954).

5. Glass, I.I. Hall, J.G. — Handbook of Supersonic Aerodynamics, Section 18, Shock Tubes, NAVORD 1488, Vol. 6, p. 1959.

6. Oppenheim, A.K. Urtiew, P.A. Laderman, A.J. — Vector Polar Method for the Evaluation of Wave Interaction Processes., Archiwum Budowy Maszyn, Vol. 11, No. 3, 1964.

7. Bird, G.A. — Extreme Temperatures in Shock-Wave Interactions with Rarefaction Waves, J. Fluid Mech, Vol. 13, p. 282 (1963).

8. Bremner, G.F. Dukowicz, J. Glass, I.I. — On the One Dimensional Overtaking of a Rarefaction Wave by a Shock Waves, ARS Journal Vol. 31, No. 10, (1959) also UTIA Technical Note No. 33, Institute of Aerophysics, University of Toronto (1960).

9. Glass, I.I. Heuckroth, L.E. Molder, E. — One Dimensional Overtaking of a Shock Wave by a Rarefaction Wave, ARS Journal, Vol. 31, No. 10, (Oct. 1961) also UTIAS Tech. Note No. 30 (1959).

10. Flagg, R.F. — Detailed Analysis of Shock Tube Tailored Conditions, Avco RAD-TM-63-64 (Sept. 1963).

11. Bull, G.V. Fowell, L.R. Henshaw, D.H. — The Interaction of Two Similarly-Facing Shock Waves, UTIA Report No. 23, Institute of Aerophysics, University of Toronto (1952).

APPENDIX A - ANALYSIS OF THE CROSS-OVER POINT

It is worthwhile to see if the point denoted as the "cross-over" point is of practical interest, for if it is, the problem of using the driver-reservoir technique is considerable simplified. The velocity u_3 in general, is related to the shock Mach number by:-

$$u_3 = a_1 \frac{2}{\gamma_1 - 1} \left(M_s - \frac{1}{M_s} \right) \tag{A-1}$$

Using M_{sx} to denote the shock Mach number for the cross-over condition and equating Eqs. (6) and (A-1) results in

$$M_{sx}^2 - 2 \frac{\gamma_1 + 1}{\gamma_4 + 1} a_{41} M_{sx} - 1 = 0 \tag{A-2}$$

The positive root provides a physical solution given by:-

$$M_{sx} = \frac{\gamma_1 + 1}{\gamma_4 + 1} a_{41} + \left[\frac{(\gamma_1 + 1)^2}{(\gamma_4 + 1)^2} a_{41}^2 + 1 \right]^{\frac{1}{2}} \tag{A-3}$$

or for the case where $a_{41} \gg 1$ (generally $M_s \gg 1$) this can be approximated by:-

$$\frac{M_{sx}}{a_{41}} \approx 2 \frac{\gamma_1 + 1}{\gamma_4 + 1} = g \tag{A-4}$$

where, g, the "cross-over constant" is defined by this equation. Equations (A-3) and (A-4) are plotted in Fig. A-1 for several specific heat ratios of interest and Eq. (A-4) is plotted in Fig. A-2 for the complete range of specific ratios of physical interest. If the shock tube is to be operated at the cross-over point a restriction is placed on the values of M_s that may be used for a given speed of sound ratio across the diaphragm.

If this constraint were the only one placed on the shock Mach number there would be no problem with using the driver reservoir as the initial conditions could be readily adjusted to yield this shock Mach number. However, in addition to the above, the shock tunnel is required to be tailored, hence, there is an additional constraint placed on the shock Mach number. Reference 10 presents the exact tailored shock Mach numbers for a wide variety of driver and driven gases and diaphragm speed of sound ratios. An exact analytic solution has not been obtained. However, for the assumption of a large shock Mach number, i.e., $M_s \gg 1$, a simple approximate expression for the tailored shock Mach number is given by (Ref. 10),

$$M_{S_T} = \text{a}_{41}\left[\frac{(\gamma_1+1)^2(\gamma_4-1) - \left[2\gamma_4(\gamma_1-1)(\gamma_4+1)(\gamma_1+1)^3\right]^{\frac{1}{2}}}{(\gamma_4-1)^2(\gamma_1+1) - 2\gamma_4(\gamma_1-1)(\gamma_4+1)}\right] \qquad \text{(A-5)}$$

Equating Eqs. (A-4) and (A-3), the approximate equations for the cross-over and tailored shock Mach numbers yields,

$$2\left[(\gamma_4-1)^2(\gamma_1+1) - 2\gamma_4(\gamma_1-1)(\gamma_4+1)\right] = (\gamma_4+1)\left\{(\gamma_4+1)(\gamma_4-1) - \left[2\gamma_4(\gamma_1-1)(\gamma_4+1)(\gamma_1+1)\right]^{\frac{1}{2}}\right\} \qquad \text{(A-6)}$$

Hence there are only certain combinations of specific heat ratios that will satisfy both the cross-over and tailoring requirements, simultaneously. For the special case of $\gamma_1 = \gamma_4$ Eq. (A-6) reduces to

$$\gamma = \frac{9}{7}$$

Equation (A-6) is plotted in Fig. A-3. Note that this figure can be used to immediately determine which category (i.e. $M_{ST} \gtrless M_{S_X}$) a given set of initial conditions falls into if M_S can be assumed large. It should be noted that the driver and reservoir gases are assumed initially at the same temperature and pressure. M_{ST} and M_{S_X} can be matched if different initial temperatures and pressures exist in the driver and the reservoir. However, this mode of operation does not appear to be a practical one since it introduces the problem of heating the driver gas and cooling the reservoir gas and adding a second diaphragm to prevent mixing different gases. Alternatively, mixtures of gases could in principle produce the same end pressures. However, an interface separating the different gases of different temperatures would give rise to an additional tailoring constraint. In general the conditions across this second interface could not be arbitrarily prescribed and hence would not be tailored simultaneously with the first interface.

Included in Fig. A-3 are the points corresponding to Helium/Air, Hydrogen/Air and Combustion/Air modes of operation. One notes that none of these combinations corresponds to the situation where the tailored shock Mach number and the cross-over shock Mach number are identical. Hence, some additional disturbances must be generated in these cases to match the two flow regimes.

TABLE 1

WAVE SYSTEMS FOR DRIVER-RESERVOIR FLOWS

System No.		Stability	Occurance
1	$\overleftarrow{R}\ C\ \overrightarrow{R}$	Stable Provided $M_{FE} \geq 1$	$M_{ST} > M_{Sx}$, $\delta_{IDEAL} > \delta > \delta_{\overrightarrow{R}}$
2	$\overleftarrow{R}\ C\ M$	Stable Provided $M_{FE} \geq 1$	$M_{ST} > M_{Sx}$, $\delta = \delta_{IDEAL}$
3	$\overleftarrow{R}\ C\ \overrightarrow{S}$	Stable Provided $M_{FE} \geq 1$	$M_{ST} > M_{Sx}$, $\delta > \delta_{IDEAL}$; $M_{ST} < M_{Sx}$, $\delta > \delta_{\overrightarrow{S}} > \delta_{IDEAL}$
4	$M\ C\ \overrightarrow{R}$	Stable	$M_{ST} > M_{Sx}$, $\delta = \delta_{\overrightarrow{R}}$
5	$M\ C\ M$	Stable	$M_{ST} = M_{Sx}$, $\delta = \delta_{IDEAL} = \delta_x$
6	$M\ C\ \overrightarrow{S}$	Stable	$M_{ST} < M_{Sx}$, $\delta = \delta_{\overrightarrow{S}}$
7	$\overleftarrow{S}\ C\ \overrightarrow{R}$	Stable Provided $M_{FE} \geq M_S'$	$M_{ST} < M_{Sx_0}$, $\delta < \delta_{IDEAL}$; $M_{ST} = M_{Sx}$, $\delta < \delta_{IDEAL}$; $M_{ST} > M_{Sx}$, $\delta < \delta_{\overrightarrow{R}} < \delta_{IDEAL}$
8	$\overleftarrow{S}\ C\ M$	Stable Provided $M_{FE} \geq M_S'$	$M_{ST} < M_{Sx}$, $\delta = \delta_{IDEAL}$
9	$\overleftarrow{S}\ C\ \overrightarrow{S}$	Stable Provided $M_{FE} \geq M_S'$	$M_{ST} < M_{Sx}$, $\delta_{\overrightarrow{S}} > \delta > \delta_{IDEAL}$

TABLE 2

CROSS-OVER AREA RATIO VERSUS DRIVER GAS SPECIFIC HEAT RATIO

1.05	.438
1.10	.430
1.15	.421
1.20	.413
1.25	.404
1.30	.396
1.35	.388
1.40	.379
1.45	.370
1.50	.362
1.55	.354
1.60	.345
1.67	.333

TABLE 3

IDEAL NOZZLE AREA RATIO FOR M_{S_T} M_{S_x}

1.1	1.1	2.0	.439	1.5	1.1	10	.362
	1.2		.441		1.2		.362
	1.3		.442		1.3		.364
	1.4		.444		1.4		.365
	1.5		.445		1.5		.367
	1.67		.446		1.67		.371
1.2	1.1	2.0	.426	1.5	1.2	∞	.362
	1.2		.428		1.3		.363
	1.3		.430		1.4		.365
	1.4		.432		1.5		.367
	1.5		.433		1.67		.370
	1.67		.435				
1.3	1.1	2.0	.413	1.57	1.1	2.0	.366
	1.2		.415		1.2		.368
	1.3		.418		1.3		.371
	1.4		.419		1.4		.373
	1.5		.421		1.5		.374
	1.67		.423		1.67		.376
1.4	1.1	2.0	.401	1.67	1.1	5.0	.334
	1.2		.403		1.2		.337
	1.3		.405		1.3		.340
	1.4		.407		1.4		.342
	1.5		.408		1.5		.346
	1.67		.410		1.67		.350
1.4	1.1	5.0	.379	1.67	1.1	10	.333
	1.67		.388		1.2		.334
1.5	1.1	2.0	.388		1.3		.337
	1.2		.390		1.4		.340
	1.3		.392		1.5		.343
	1.4		.394		1.67		.347
	1.5		.396	1.68	1.2	∞	.334
	1.67		.398		1.3		.336
1.5	1.1	5.0	.362		1.4		.339
	1.2		.363		1.5		.342
	1.3		.365		1.67		.346
	1.4		.368				
	1.5		.370				
	1.67		.374				

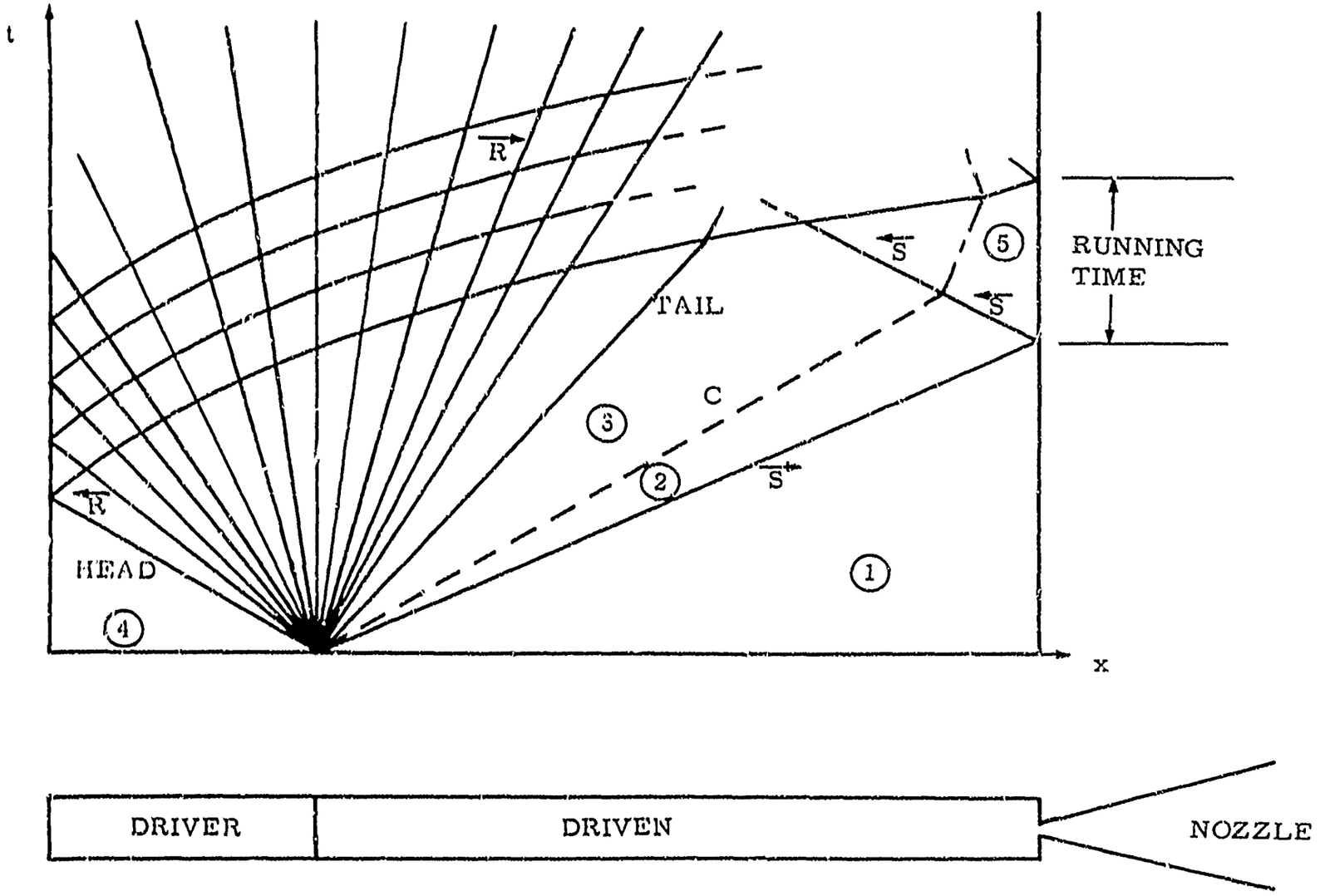

FIGURE 1 CONVENTIONAL SHOCK TUNNEL x-t DIAGRAM

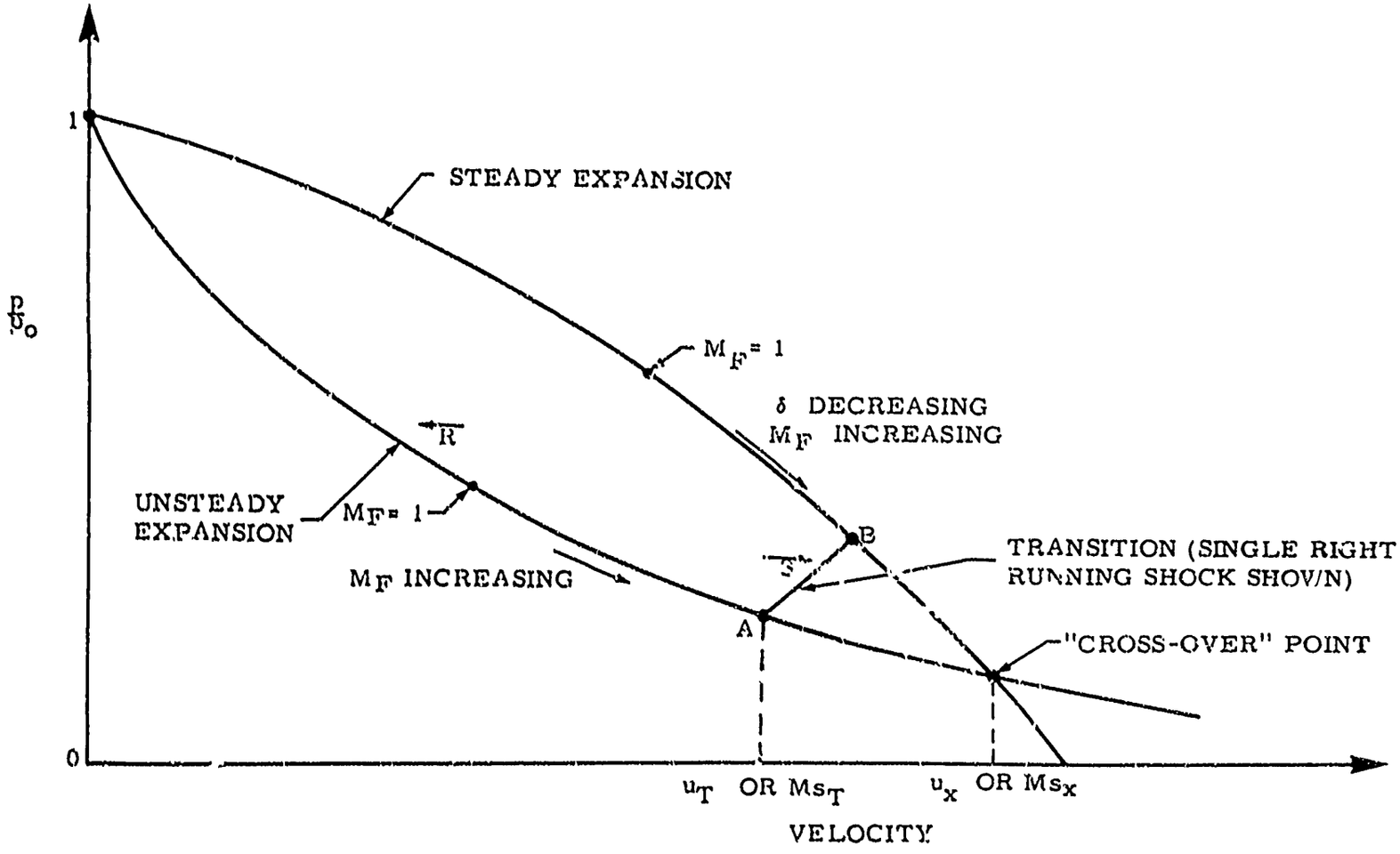

FIGURE 3 CHARACTERISTICS OF STEADY AND UNSTEADY EXPANSIONS ON THE (p, u) -PLANE

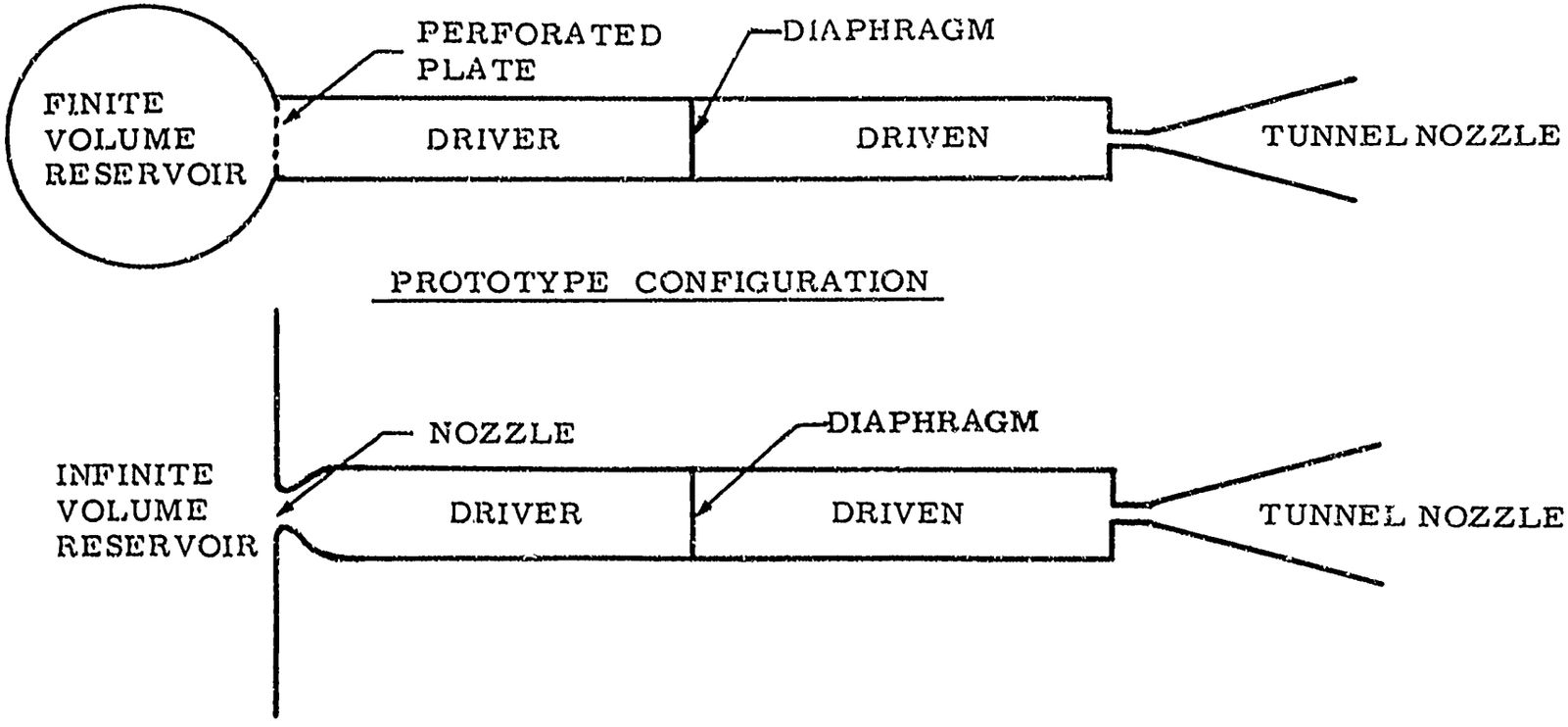

FIGURE 2 PROTOTYPE AND PHYSICAL MODEL OF DRIVER RESERVOIR

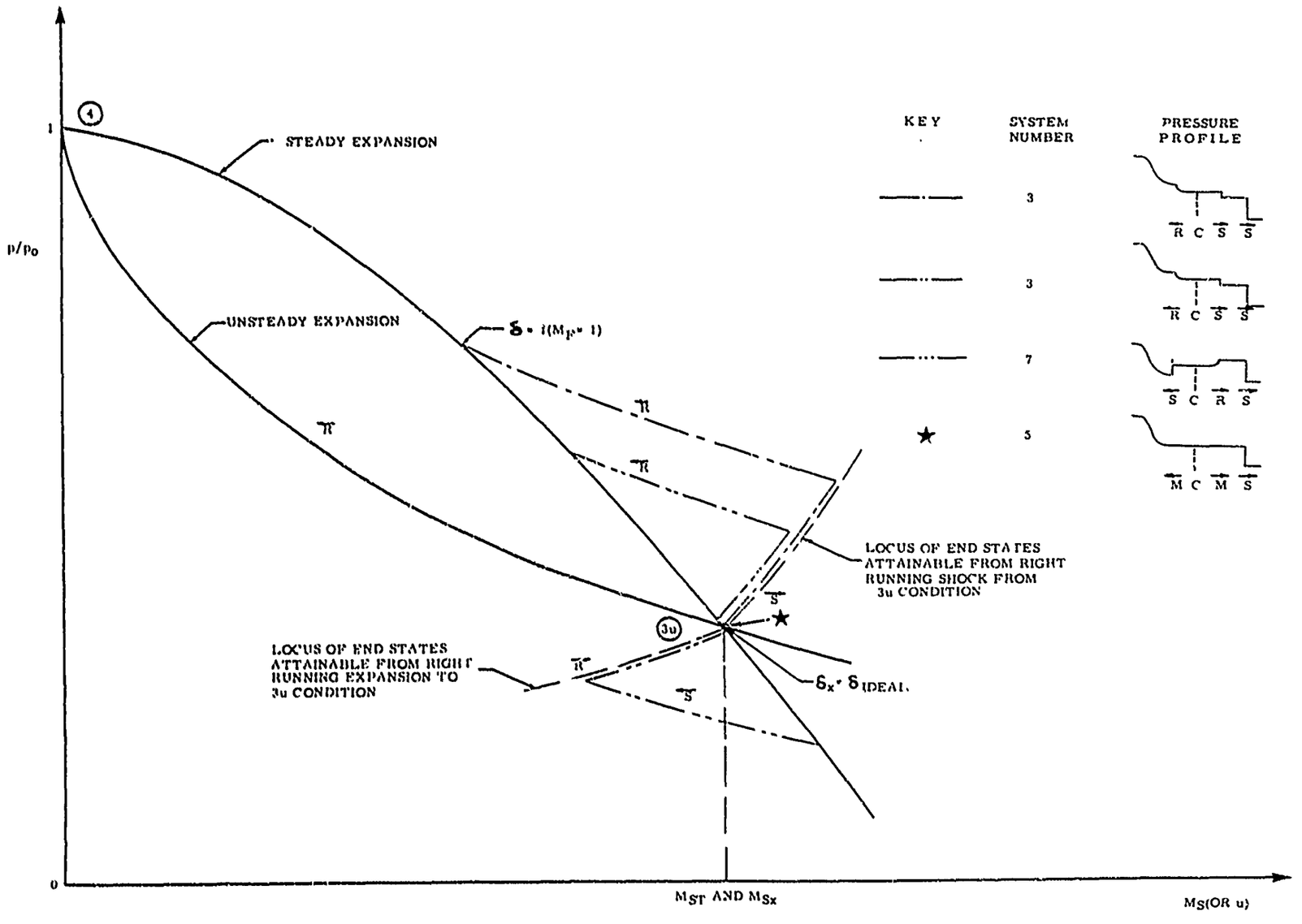

FIGURE 5 PRESSURE - VELOCITY PLANE TRACES OF WAVE SYSTEMS FOR $M_{ST}/M_{Sx} = 1$

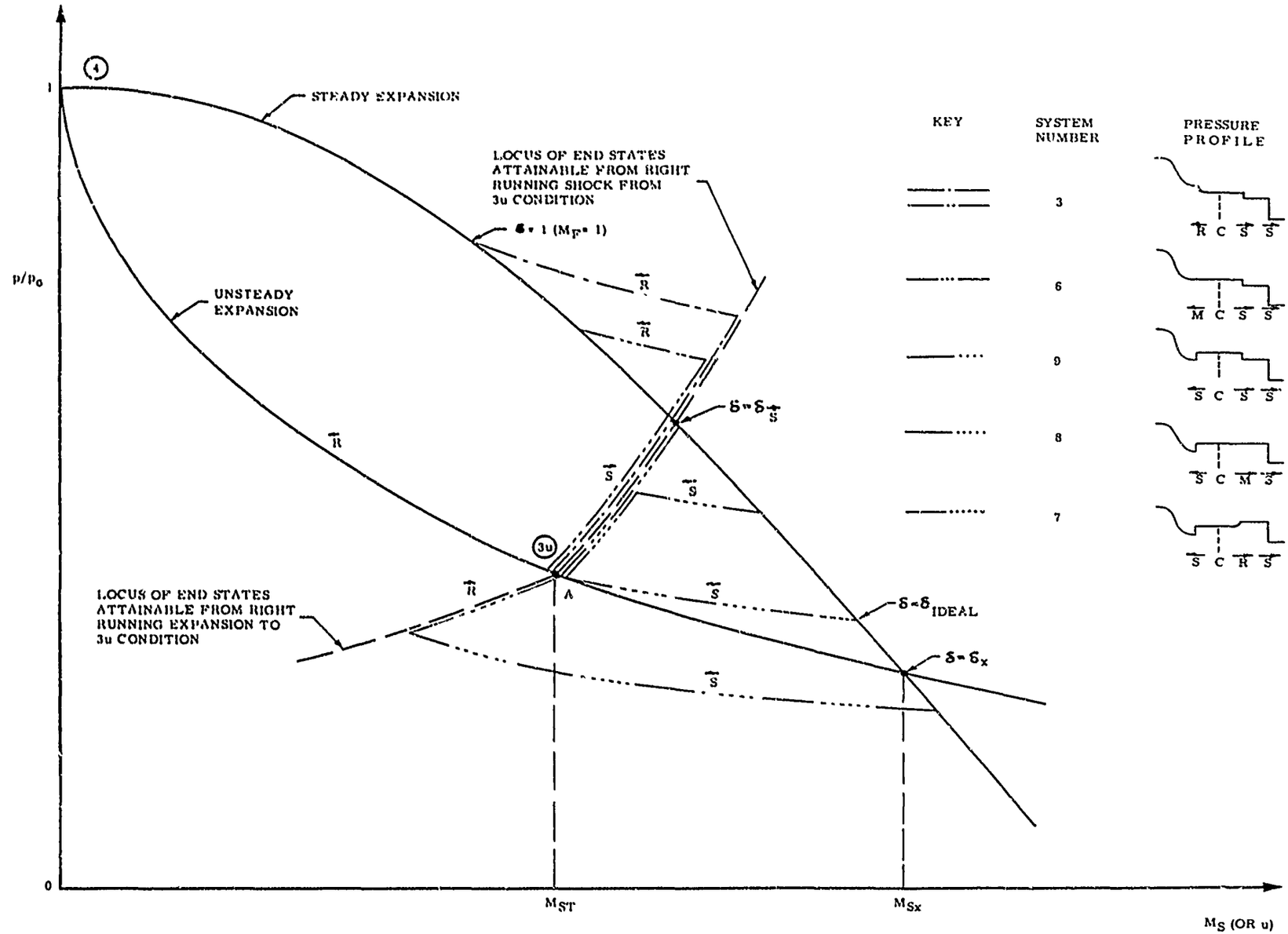

FIGURE 4 PRESSURE - VELOCITY PLANE TRACES OF WAVE SYSTEMS FOR $M_S/M_{Sx} < 1$

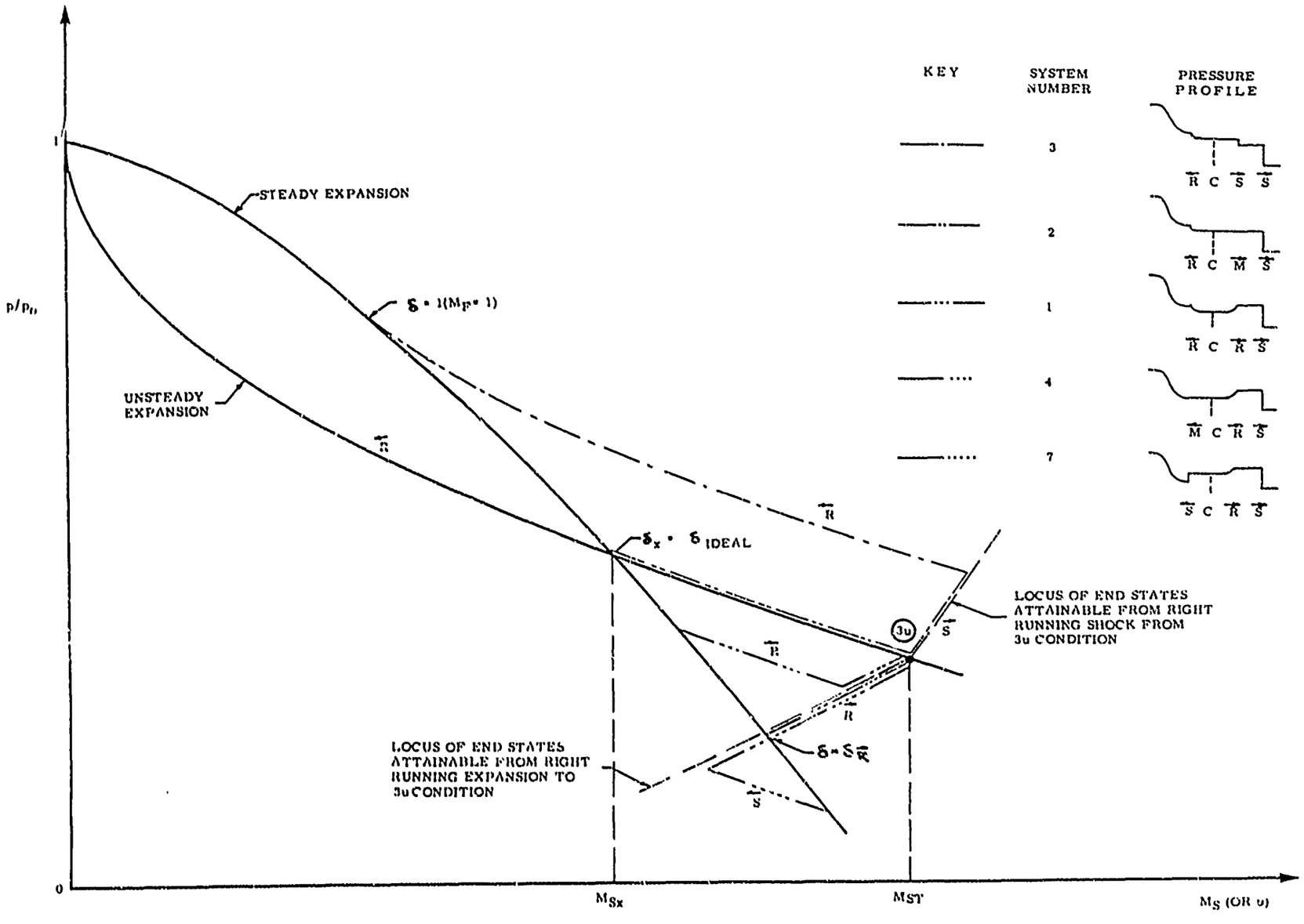

FIGURE 6 PRESSURE - VELOCITY PLANE TRACES OF WAVE SYSTEMS FOR $M_{ST}/M_{Sx}>1$

FIGURE 7

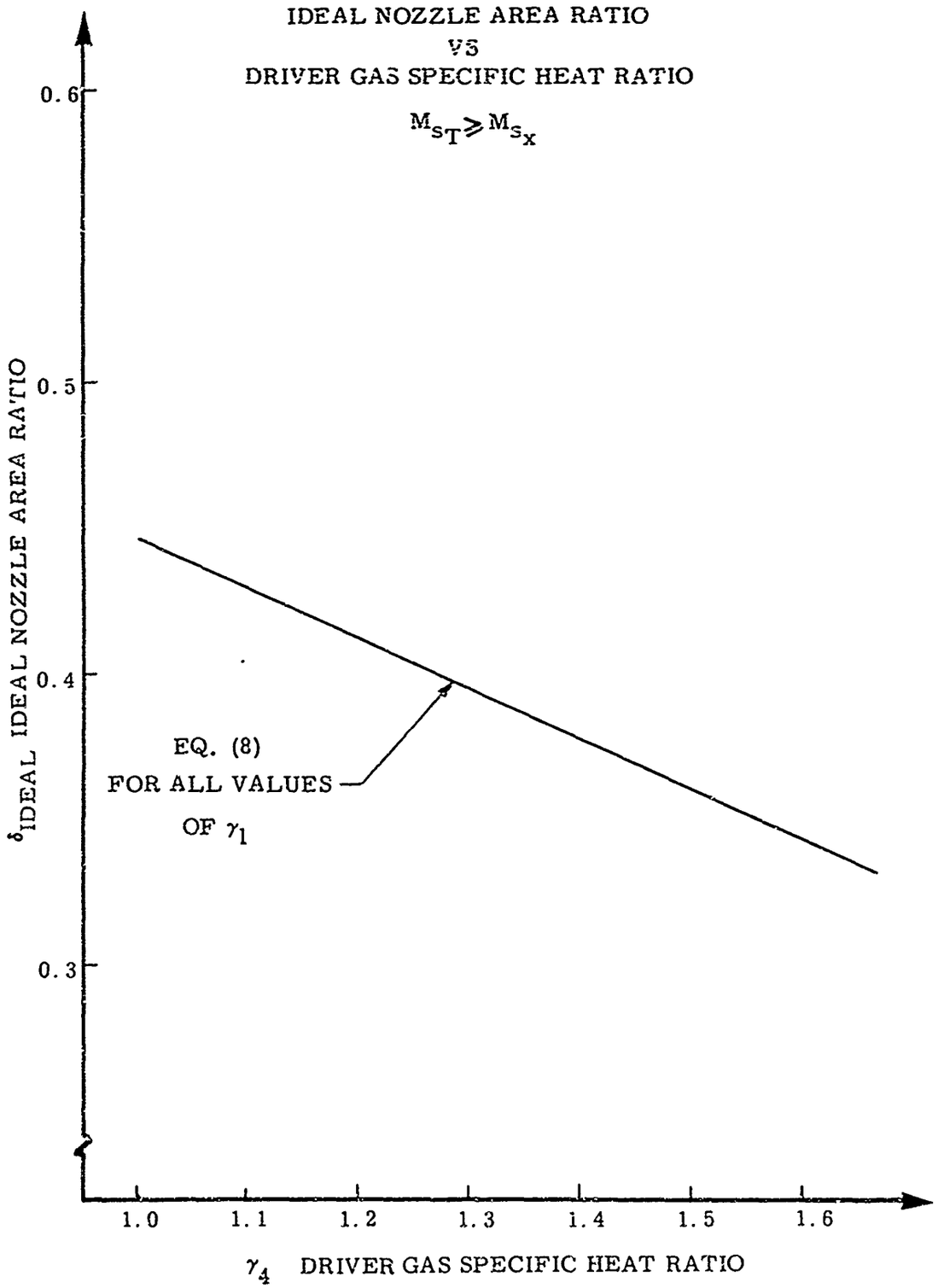
IDEAL NOZZLE AREA RATIO
VS
DRIVER GAS SPECIFIC HEAT RATIO
$M_{S_T} \geq M_{S_x}$
0.6
0.5
0.4
0.3
δ_{IDEAL} IDEAL NOZZLE AREA RATIO
EQ. (8)
FOR ALL VALUES
OF γ_1
1.0
1.1
1.2
1.3
1.4
1.5
1.6
γ_4 DRIVER GAS SPECIFIC HEAT RATIO

FIGURE 8
IDEAL NOZZLE AREA RATIO VS
DRIVEN GAS SPECIFIC HEAT RATIO

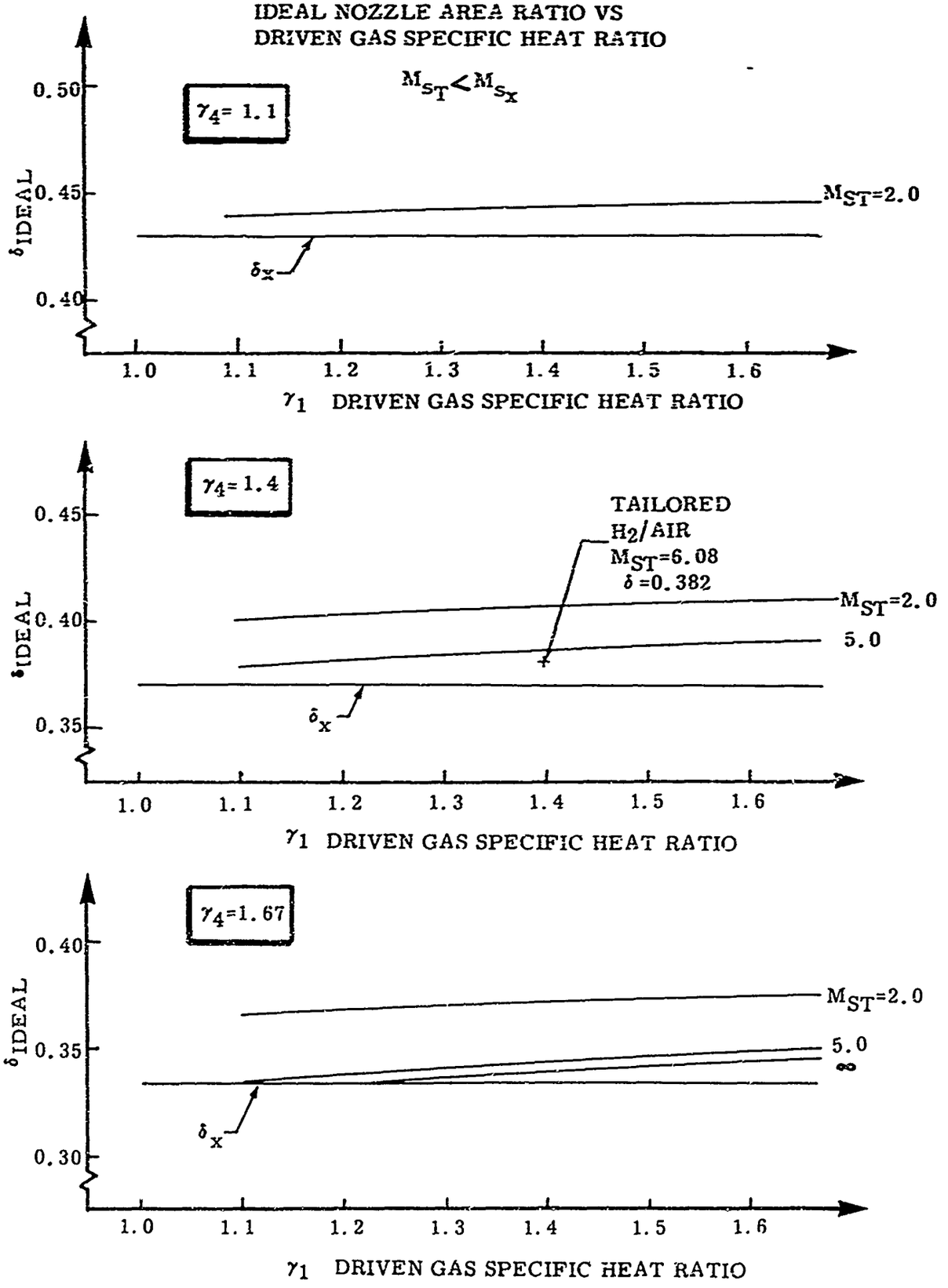

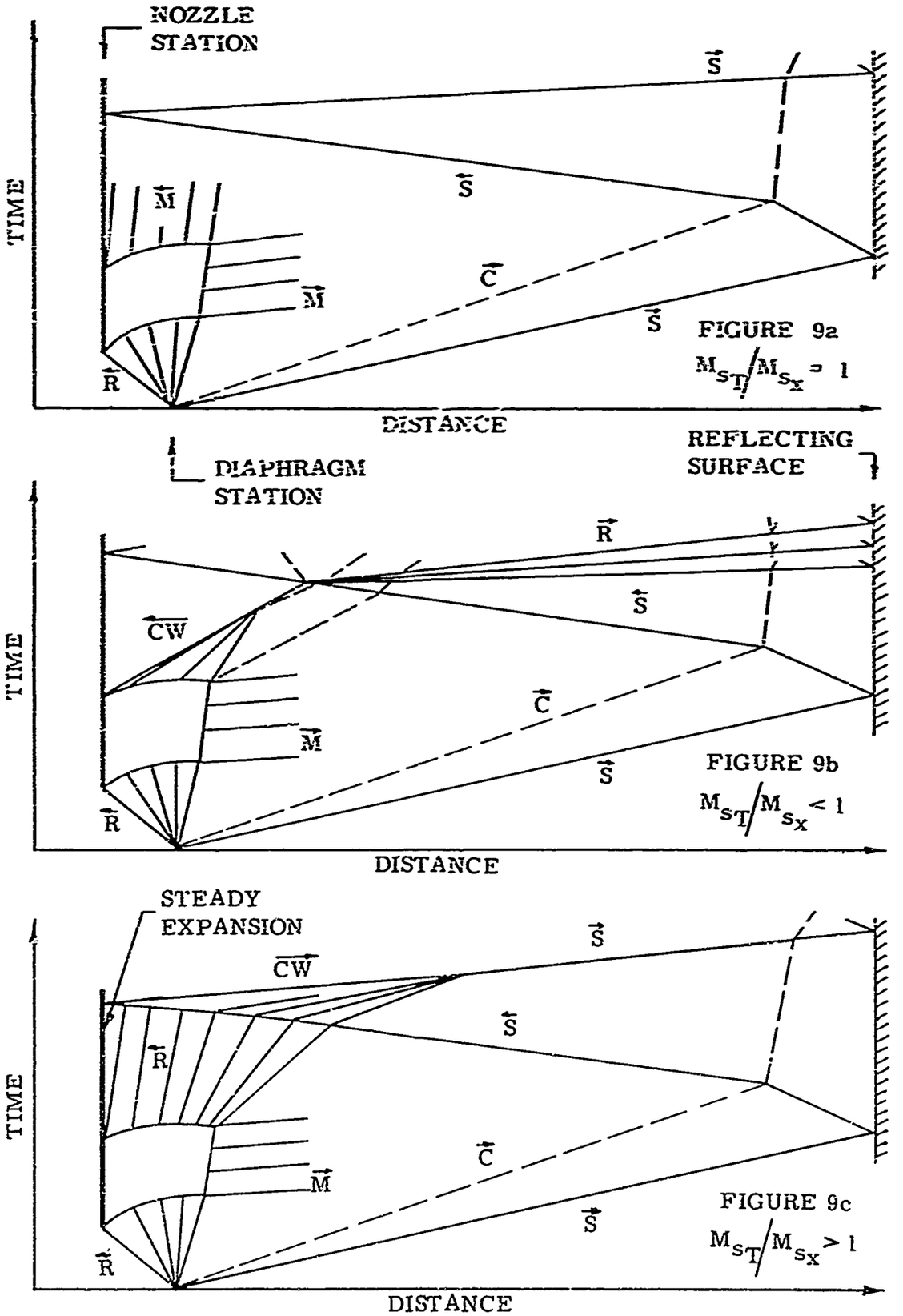

FIGURE 9 WAVE DIAGRAMS FOR LIMITING DRIVER-RESERVOIR FLOWS

FIGURE A 1

CROSS OVER SHOCK MACH NUMBER
VS
DIAPHRAGM SPEED OF SOUND RATIO

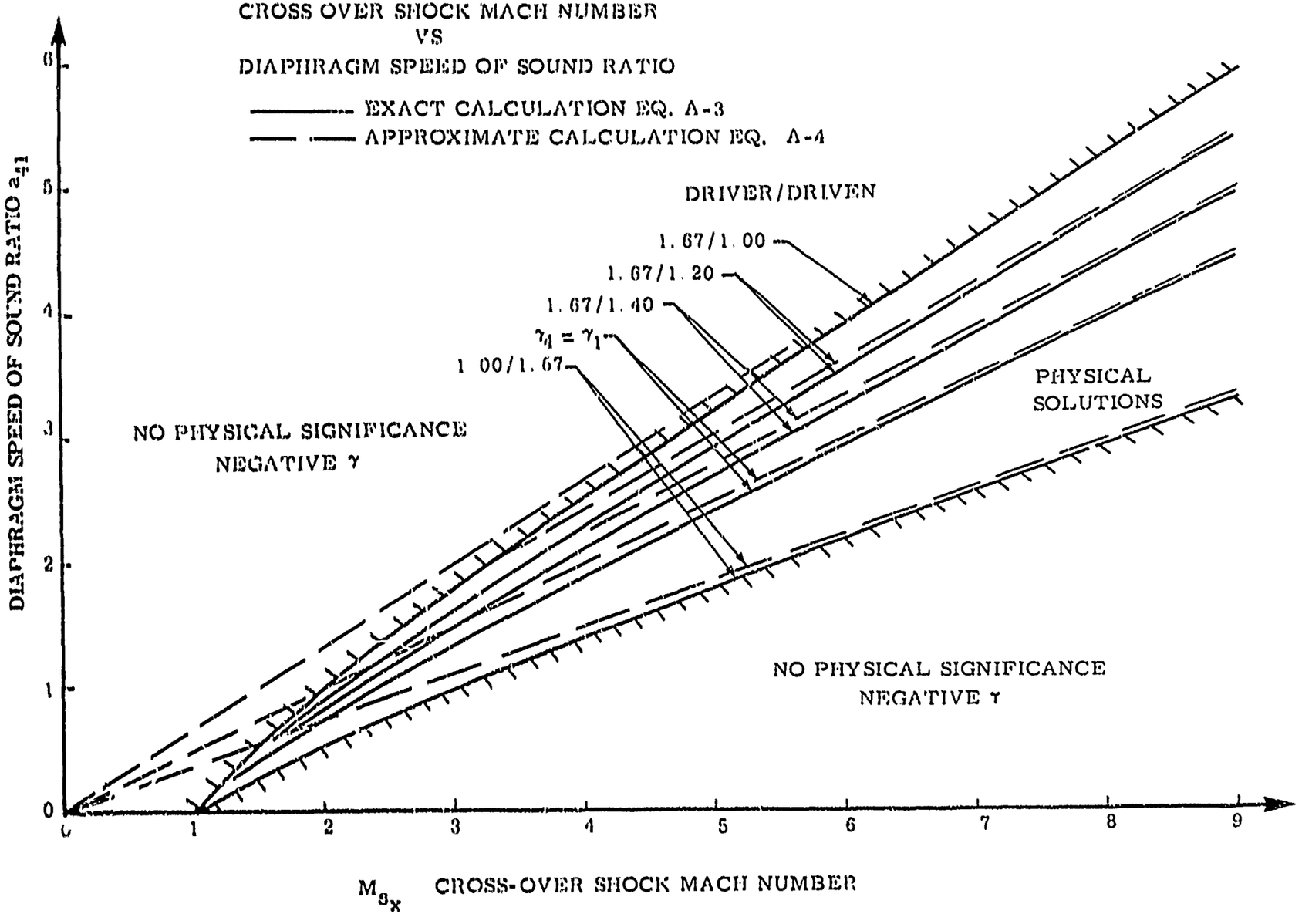

FIGURE A-2
CROSS OVER CONSTANT
VS
DRIVEN GAS RATIO OF SPECIFIC HEATS
γ_4 AS PARAMETER
$M_S \gg 1$

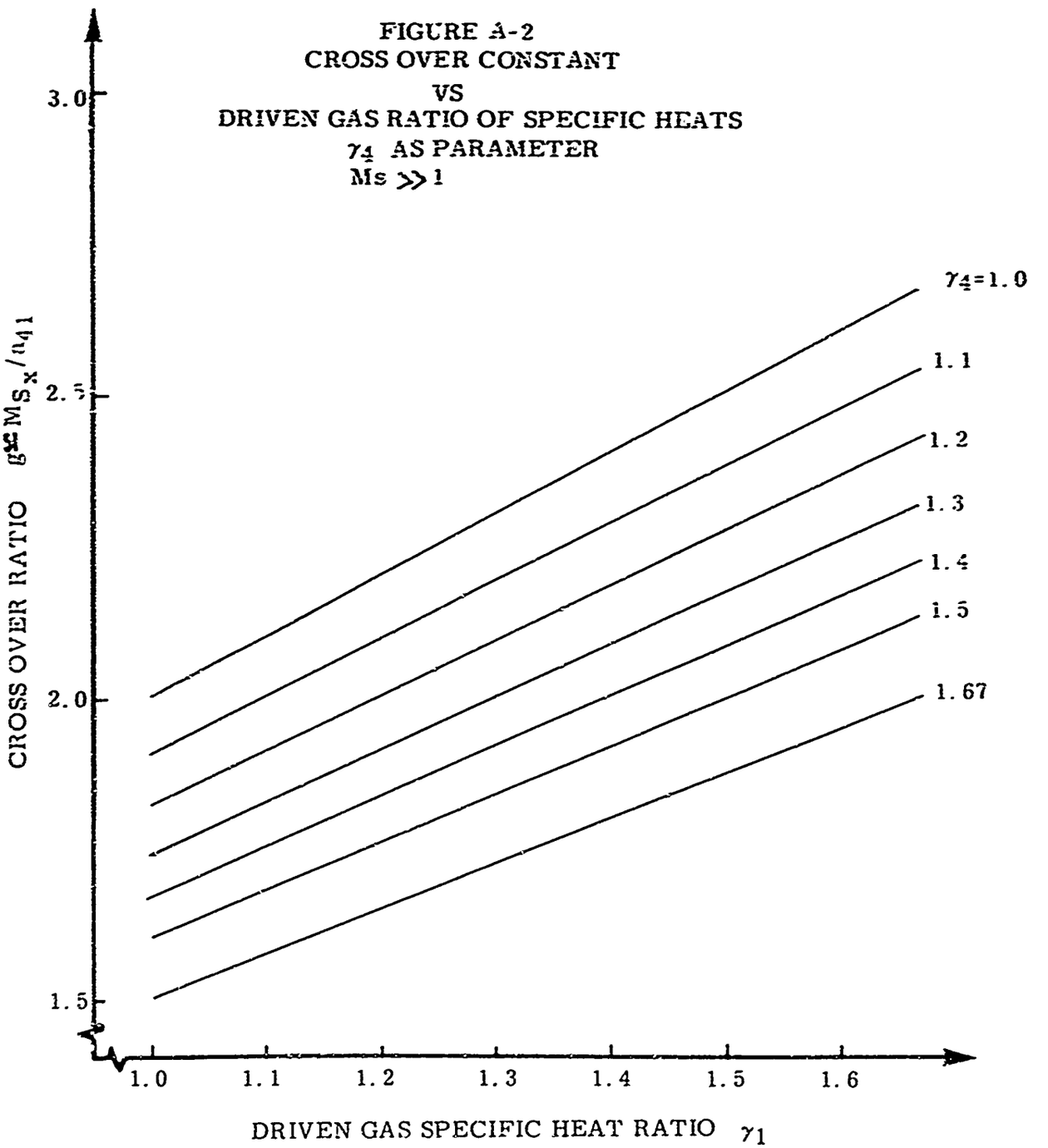

FIGURE A-3
RATIO OF SPECIFIC HEAT COMBINATIONS
THAT YIELD $M_{ST} = M_{S_X}$ FOR $M_S \gg 1$